Chaos, Solitons and Fractals 79 (2015) 130–144

Contents lists available at ScienceDirect

Chaos, Solitons and Fractals

Nonlinear Science, and Nonequilibrium and Complex Phenomena

journal homepage: www.elsevier.com/locate/chaos

Entry limitations and heterogeneous tolerances in a Schelling-like segregation model

Davide Radi [a,*], Laura Gardini [b]

[a] Department of Management, Polytechnic University of Marche, Ancona, Italy
[b] DESP, University of Urbino Carlo Bo, Urbino, Italy

ARTICLE INFO

Article history:
Available online 10 August 2015

Keywords:
Schelling's models
Border collision bifurcations
Piecewise smooth maps

ABSTRACT

In this paper we consider a Schelling-type segregation model with two groups of agents that differ in some aspects, such as religion, political affiliation or color of skin. The first group is identified as the local population, while the second group is identified as the newcomers, whose members want to settle down in the city or country, or more generally a system, already populated by members of the local population.

The members of the local population have a limited tolerance towards newcomers. On the contrary, some newcomers, but not all of them, may stand the presence of any amount of members of the local population. The heterogeneous, and partially limited, levels of tolerance trigger an entry and exit dynamics into and from the system of the members of the two groups based on their satisfaction with the number of members of the other group into the system. This entry/exit dynamics is described by a continuous piecewise-differentiable map in two dimensions. The dynamics of the model is characterized by smooth bifurcations as well as by border collision bifurcations. A combination of analytical results and numerical analysis are the main tools used to describe the quite complicated local and global dynamics of the model. The investigation reveals that two factors are the main elements that preclude integration. The first one is a low level of tolerance of the members of the two populations. The second one is an excessive and unbalanced level of tolerance between the two populations. In this last case, to facilitate the integration between members of the two groups, we impose an entry-limitation policy represented by the imposition of a maximum number of newcomers allowed to enter the system. The investigation of the dynamics reveals that the entry-limitation policy is useful to promote integration as it limits the negative effects due to excessive and unbalanced levels of tolerance.

1. Introduction

In real-world situations, the integration of people who differ for religion, color of skin, political opinions and any other element of diversity is a complicated aspect that has many implications and affects all aspects of the human being's life and of the global society in general, such as personal relations, social relations, economics, politics, and the like. The main cause of non-integration (or segregation) is the limited level of tolerance that groups of individuals who share ideals, or are characterized by common features, have towards individuals that do not belong to their cluster. Moreover, the assumption that residential segregation observable in many U.S. cities, see, e.g. [1], is the output of a free interaction of agents guided by their own discriminatory individual choices, leads someone to think that individuals are totally intolerant. Nevertheless, other ones can be the causes leading

* Corresponding author. Tel.: +39 328 3561 091.
E-mail addresses: d.radi@univpm.it (D. Radi), laura.gardini@uniurb.it (L. Gardini).

http://dx.doi.org/10.1016/j.chaos.2015.07.009
0960-0779/

to segregation. As underlined earlier by Schelling, see [2] and [3], and more recently in [1], [4], [5] and [6], a deep investigation of the real situation reveals that the segregation in many U.S. cities does not reflect the desire of the people but is the result of sets of integration preferences of the members of the different groups that are limited and mutually incompatible.

In his seminal contribution, see [2], Schelling proposes (sketches) two models to represent and describe the issue. The first model is a primeval example of agent-based modeling[1] that takes into account the point of view and the decisions of every single individual involved. This model has been extended and analyzed in many contributions, see e.g. [7,8] and [9]. The second model is a two-dimensional dynamical system that describes the entry/exit dynamics of the members of two populations in a city or a country or more generally a system. This model considers individuals as members of the two groups and describes the aggregate dynamics to result from the interaction of the two groups and based on adaptive mechanisms. Recently, see [10,11]–[12], this second model has been proposed as a nonlinear two-dimensional map. Compared to the agent-based models, this second setup allows us to base the findings of the dynamics of segregation on a solid mathematical ground and to use the last developments of the bifurcation theory, especially border collision bifurcation theory, to describe the mechanisms that either lead to segregation or promote integration. Nevertheless, the second setup does not have the flexibility and the possibility to detail the preferences and the differences, especially in terms of level of tolerance, of each single agent. However, it can be used as a solid mathematical validation of the results of the more general agent-based models and can offer a valid interpretation of some of the phenomena, at first sight unexplainable, that can result due to the nonlinearity of the entry/exit dynamics.

These Schelling-type models are mainly based on the simple assumption of homogeneous distributions of tolerances of members of different groups. However, this is not always the case in real-world situations where the heterogeneity of the distributions of tolerances is a crucial aspect of the segregation dynamics. An empirical analysis conducted in the U.S.A. to study the propensity of individuals of different ethnic groups to live together in the same neighborhood reveals distributions of tolerance of different shapes for the different ethnic groups, see [1]. The main difference in the distributions of tolerance among ethnic groups is related to the maximum number of agents of the other groups that are tolerated. In particular, from the empirical results reported and commented in [1], it emerges that some ethnic groups are characterized by a small fraction of individuals that can stand the presence of any number of individuals of the other groups, while some other ethnic groups can stand only a limited number of individuals of the other groups.

With the aim of capturing and describing the effect of this heterogeneity, we imagine a city or a country populated by two groups of individuals. One group is the local population, which is characterized by a limited level of tolerance and the second group are newcomers, which are characterized by a subgroup of members that tolerate the presence of any number of members of the other group. We normalize to one the number of individuals of the local population and we assume that the newcomers are in fewer numbers than the individuals of the local population. The resulting tolerance distributions and the adaptive dynamics describing the entry/exit flows of the members of the local population and of the members of the newcomers are similar to the one proposed in [10].

The analysis of the model reveals that for both low levels and large levels of tolerances the segregation equilibria represent the only asymptotically stable fixed points of the model. On the contrary, for intermediate levels of tolerance an equilibrium of non-segregation can be asymptotically stable. However, this equilibrium always coexists with at least another asymptotically stable equilibrium of segregation.

The results can partially appear counter-intuitive, especially the fact that the dynamic investigation of the model reveals that segregation can be caused by an excess of tolerance. Nevertheless, this phenomenon has a simple and straightforward explanation in terms of mutually incompatible sets of preferences as suggested by Schelling. Indeed, the high levels of tolerance of newcomers, which combined with the high, but in any case limited, tolerance levels of the individuals of the local population, boost the first ones to enter in a massive way and force the last ones to leave the city or the country where they live.

In order to provide a valid solution to the segregation caused by large levels of tolerances, we introduce entry-limitation constraints which apply to the newcomers. These entry restrictions represent an entry-limitation policy imposed by regulators that turns out to promote integration between individuals of the two populations. Indeed, such an exogenous control reduces the risk of massive entry and exit dynamics, typical of emotional or impulsive reactions, resulting from unbalanced levels of tolerance between members of the local population and newcomers, that threaten the possibility to have integration. For obvious reasons, the entry-limitations can be imposed only to the newcomers. Indeed, it is difficult to imagine that a regulator can force part of the local population to leave the region in which it lives and moves to another place for the sake of integration.

Due to the introduction of the entry-limitations a new asymptotically stable equilibrium of integration (or non-segregation) can appear through a border collision bifurcation. Moreover, the entry-limitations have the effect of reducing the amount of chaos in the dynamics of the system. This occurs through a sequence of border collision bifurcations. Indeed, the entry-limitations have the effect of introducing a further curve of non-differentiability in a map that is already piecewise differentiable.

This characteristic of the map makes the model interesting also from a mathematical point of view. Indeed, the investigation reveals the existence of *border collision bifurcations*, see e.g. [13–30] and [31] for theory and applications in economics and social sciences, both of codimension-one and codimension-two, which combined with smooth bifurcations of different types (as saddle-node bifurcations and

[1] As suggested by an anonymous referee, Schelling's contribution is defined by Epstain and Axtell, see [7], as "an early and prescient example of agent-based modeling in the social sciences".

sequences of flip, or period doubling, bifurcations), see e.g. [32], generate complex dynamics.

The paper is organized as follows. Section 2 introduces the model and some of its general properties. Section 3 identifies the possible fixed points of the model, and the bifurcations leading to their existence, providing results about their asymptotic stability and investigates the possible bifurcations of the fixed points themselves. Section 4 describes the global dynamics of the model without entry-limitations by means of numerical tools and analytical results. Section 5 investigates the effect of the entry limitations. Section 6 concludes.

2. The model setup

Let us consider a neighborhood, or a district, populated by agents belonging to two groups denoted as local population and the newcomers. The members of these two groups decide to enter or exit the neighborhood according to their level of satisfaction, which depends on the number of members of the other group currently present in the neighborhood itself. Let us denote by x_1 and by x_2 the number of members of the local population and of the newcomers, respectively, that live in the neighborhood. Specifically, the entry and exit dynamics is regulated by a simple adjusted mechanism according to which members of both groups exit the neighborhood when the presence of the members of the other group exceeded the maximum tolerated number and enter otherwise. The speed at which the entry and exit dynamics occur is regulated by an adjustment parameter, here indicated by γ_1 for the local population and by γ_2 for the newcomers, that we assume to depend on the socioeconomic conditions of the residential area (or neighborhood, or district) at stake. For example, housing market conditions can speed up or slow down the movements of people in and out of the neighborhood. The entry and exit dynamics can be formalized in a dynamical model. In particular, the modeling framework to analyze is the following piecewise smooth two-dimensional map $(x_1', x_2') = T(x_1, x_2)$ defined as follows:

$$T: \begin{cases} x_1' = \begin{cases} 0 & \text{if } F_1(x_1,x_2) \le 0 \\ F_1(x_1,x_2) & \text{if } 0 \le F_1(x_1,x_2) \le N_1 \\ N_1 & \text{if } F_1(x_1,x_2) \ge N_1 \end{cases} \\ x_2' = \begin{cases} 0 & \text{if } F_2(x_1,x_2) \le 0 \\ F_2(x_1,x_2) & \text{if } 0 \le F_2(x_1,x_2) \le K_2 \\ K_2 & \text{if } F_2(x_1,x_2) \ge K_2 \end{cases} \end{cases} \tag{1}$$

with

$$\begin{aligned} F_1(x_1,x_2) &= x_1[1+\gamma_1(x_1R_1(x_1)-x_2)] \\ F_2(x_1,x_2) &= x_2[1+\gamma_2(x_2R_2(x_2)-x_1)] \end{aligned} \tag{2}$$

and

$$\begin{aligned} R_1(x_1) &= \tau_1\left(1-\frac{x_1}{N_1}\right) \\ R_2(x_2) &= \tau_2\left(\frac{N_2}{x_2}-1\right) \end{aligned} \tag{3}$$

where N_1 represents the size of the local population, which we assume to be the larger of the two, and we normalize to one, i.e. $N_1 = 1$. The numerosity of the second population, the newcomers, is indicated by N_2 and for obvious reasons it is assumed to be smaller than the local population. Normalizing the size of population two to the size of the local population, we have that

$$0 < N_2 \le N_1 (= 1). \tag{4}$$

The two functions $R_i(x_i)$ represent the level of tolerance of the two populations that depend on the level-of-tolerance parameters τ_i. In particular, the maximum number of members of the newcomers (of the local population) tolerated by x_1 (x_2) members of the local population (of the newcomers) is given by $x_1R(x_1)$ ($x_2R(x_2)$).

The first tolerance function R_1 is based on the assumption that members of the local population have heterogeneous and limited degrees of tolerance. On the contrary, the tolerance function of newcomers' population is based on the fact that a small part of the members of this population is not disturbed by the presence of the other population and can bear any number of people of the other population living in their own neighborhood. This modeling choice is supported by empirical evidence, see [1].

The unlimited entry of newcomers in a neighborhood can generate the reaction of the local population, that can decide to move to another neighborhood. This can boost an entry-exit dynamics in the system that can be described by means of an adjustment mechanism as the one indicated by the map T in (1).

The rulers can decide to limit the entry of the newcomers imposing entrance limitations for them. In order to understand the possible effects of this "anti-segregation policy", we introduce a constraint, represented by the parameter K_2 with

$$0 < K_2 \le N_2 \tag{5}$$

which allows newcomers to enter the neighborhood only in a limited number.

As indicated above, the parameters $\gamma_1(>0)$ and $\gamma_2(>0)$ indicate how fast each population reacts to the tolerated/non-tolerated levels of members of the other population entering/exiting the neighborhood. We assume that this reactivity depends on real estate or housing market conditions, labor flexibility, local bureaucracy and municipality and so we are led to assume the same value for both the populations, i.e. $\gamma = \gamma_1 = \gamma_2$. We also assume that the tolerance parameters are positive, thus

$$\gamma > 0, \quad \tau_1 > 0, \quad \tau_2 > 0. \tag{6}$$

In explicit form the functions F_i defining map T are as follows:

$$\begin{aligned} F_1(x_1,x_2) &= x_1\left[1+\gamma\left(x_1\tau_1\left(1-\frac{x_1}{N_1}\right)-x_2\right)\right] \\ F_2(x_1,x_2) &= x_2[1+\gamma(\tau_2N_2-\tau_2x_2-x_1)]. \end{aligned} \tag{7}$$

From the definition of map T it is clear that any point of the plane in one iteration is mapped in the rectangle D given by

$$D = [0, N_1] \times [0, K_2] \tag{8}$$

and an orbit cannot escape from it. Moreover, the range D of the map is divided in several regions, whose shape and size depend on the parameters. In the different regions the system changes its definition, although continuously. The

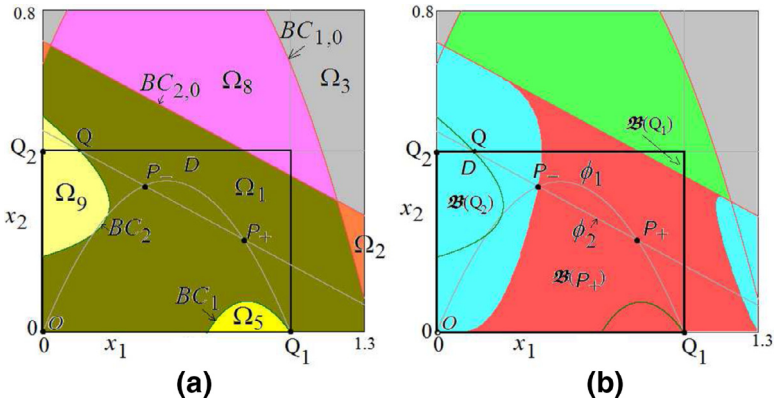

Fig. 1. Phase space of map T, and range D marked, for the following values of the parameters: $\gamma = 1.5$, $\tau_1 = 1.5$, $\tau_2 = 3$, $N_1 = 1$, $N_2 = 0.5$ and $K_2 = 0.45$. Panel (a), some regions Ω_i. Panel (b), representation of the fixed points and their basins of attractions. In green the basin of attraction of the fixed point of segregation Q_1. In azure the basin of attraction of the fixed point of segregation Q_2. In red the basin of attraction of the natural fixed point of non-segregation P_+. In gray is the basin of attraction of fixed point O. (For interpretation of the references to color in this figure legend, the reader is referred to the web version of this article.)

boundaries of these regions are sets of non-differentiability for map T and are defined by the following curves:

$$\begin{aligned} BC_1 : x_2 &= \frac{1}{\gamma}\left[1 + \gamma x_1 R_1(x_1) - \frac{N_1}{x_1}\right] \\ &= \frac{1}{\gamma} + \tau_1 x_1\left(1 - \frac{x_1}{N_1}\right) - \frac{N_1}{\gamma x_1} \\ &\quad \text{where } F_1(x_1, x_2) = N_1 \\ BC_2 : \ x_1 &= \frac{1}{\gamma}\left[1 + \gamma x_2 R_2(x_2) - \frac{K_2}{x_2}\right] \\ &= \frac{1}{\gamma} + \tau_2(N_2 - x_2) - \frac{K_2}{\gamma x_2} \\ &\quad \text{where } \ F_2(x_1, x_2) = K_2 \end{aligned} \tag{9}$$

and by the curves $F_i(x_1, x_2) = 0$ which, as it is immediate, are given by $x_i = 0$, and two more curves given by:

$$\begin{aligned} BC_{1,0} : \ x_2 &= \frac{1}{\gamma}[1 + \gamma x_1 R_1(x_1)] = \frac{1}{\gamma} + \tau_1 x_1\left(1 - \frac{x_1}{N_1}\right) \\ &\quad \text{where } \ F_1(x_1, x_2) = 0, \ x_1 \neq 0 \\ BC_{2,0} : \ x_1 &= \frac{1}{\gamma}[1 + \gamma x_2 R_2(x_2)] = \frac{1}{\gamma} + \tau_2(N_2 - x_2) \\ &\quad \text{where } \ F_2(x_1, x_2) = 0, \ x_2 \neq 0. \end{aligned} \tag{10}$$

An example is shown in Fig. 1a.

The curves of non-differentiability defined in (9) and (10) divide the phase plane into the following nine regions:

$$\begin{aligned} \Omega_1 &= \{(x_1, x_2) | 0 \le F_1(x_1, x_2) \le N_1 \text{ and } 0 \le F_2(x_1, x_2) \le K_2\} \\ \Omega_2 &= \{(x_1, x_2) | F_1(x_1, x_2) \le 0 \text{ and } 0 \le F_2(x_1, x_2) \le K_2\} \\ \Omega_3 &= \{(x_1, x_2) | F_1(x_1, x_2) \le 0 \text{ and } F_2(x_1, x_2) \le 0\} \\ \Omega_4 &= \{(x_1, x_2) | F_1(x_1, x_2) \le 0 \text{ and } F_2(x_1, x_2) \ge K_2\} \\ \Omega_5 &= \{(x_1, x_2) | F_1(x_1, x_2) \ge N_1 \text{ and } 0 \le F_2(x_1, x_2) \le K_2\} \\ \Omega_6 &= \{(x_1, x_2) | F_1(x_1, x_2) \ge N_1 \text{ and } F_2(x_1, x_2) \le 0\} \\ \Omega_7 &= \{(x_1, x_2) | F_1(x_1, x_2) \ge N_1 \text{ and } F_2(x_1, x_2) \ge K_2\} \\ \Omega_8 &= \{(x_1, x_2) | 0 \le F_1(x_1, x_2) \le N_1 \text{ and } F_2(x_1, x_2) \le 0\} \\ \Omega_9 &= \{(x_1, x_2) | 0 \le F_1(x_1, x_2) \le N_1 \text{ and } F_2(x_1, x_2) \ge K_2\} \end{aligned} \tag{11}$$

also shown in Fig. 1a, in each of which, as remarked above, map T takes a different definition, given explicitly as follows:

$$\begin{aligned} (x_1, x_2) \in \Omega_1 &: (x_1', x_2') = (F_1(x_1, x_2), F_2(x_1, x_2)) \\ (x_1, x_2) \in \Omega_2 &: (x_1', x_2') = (0, F_2(x_1, x_2)) \\ (x_1, x_2) \in \Omega_3 &: (x_1', x_2') = (0, 0) \\ (x_1, x_2) \in \Omega_4 &: (x_1', x_2') = (0, K_2) \\ (x_1, x_2) \in \Omega_5 &: (x_1', x_2') = (N_1, F_2(x_1, x_2)) \\ (x_1, x_2) \in \Omega_6 &: (x_1', x_2') = (N_1, 0) \\ (x_1, x_2) \in \Omega_7 &: (x_1', x_2') = (N_1, K_2) \\ (x_1, x_2) \in \Omega_8 &: (x_1', x_2') = (F_1(x_1, x_2), 0) \\ (x_1, x_2) \in \Omega_9 &: (x_1', x_2') = (F_1(x_1, x_2), K_2) \end{aligned} \tag{12}$$

and since the map is continuous, at a border point between two different regions the applied functions take the same value.

3. Fixed points of the model

Regarding the fixed points of the map, satisfying $T(x_1, x_2) = (x_1, x_2)$, as we shall see in this section, we have to take into account the possible internal fixed points, which we call "natural fixed points of non-segregation", as the fixed points P_- and P_+ showed in Fig. 1b, as well as constrained fixed points, belonging to the boundary of the range D. These constrained fixed points are of two different kinds: those which belong to the coordinate axes, and thus represent the extinction of one population, as the fixed points Q_1 and Q_2 in Fig. 1b, which are called "fixed points of segregation" among which we also have to include the origin $O = (0, 0)$ which is a "fixed point of extinction", and a second kind belonging to the upper border of the rectangle D, as the points $\overline{P}_-$ and $\overline{P}_+$ in Fig. 2, which are called "artificial fixed points of non-segregation".

Summarizing, in this section we are going to determine the conditions for the existence of all the possible fixed points of the segregation model in (1), each of which has a specific socioeconomic meaning, and are classified as in the following definition:

Definition 1. The possible fixed points of map T are denoted

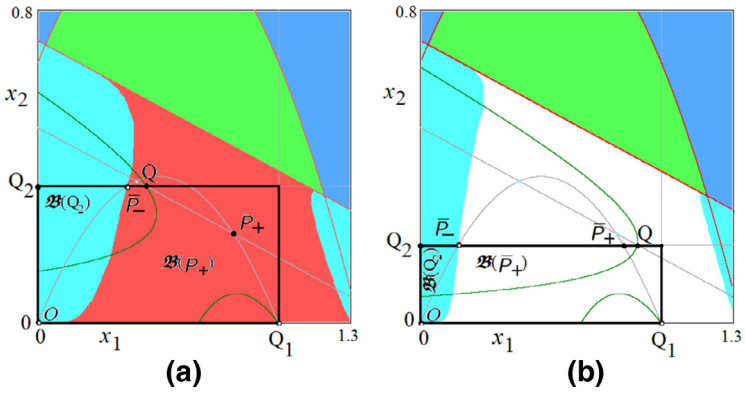

Fig. 2. Phase space of map T, and range D for the values of the parameters as in Fig. 1 and $K_2 = 0.35$ in (a), $K_2 = 0.2$ in (b). The colors of the basins have the same meaning as in Fig. 1, and in white the basin of attraction of $\overline{P}_+$.

1. Q_1 and Q_2: " fixed points of segregation";
2. P_- and P_+ : "natural fixed points of non-segregation";
3. $\overline{P}_-$ and $\overline{P}_+$: "artificial fixed points of non-segregation";
4. O: "fixed point of extinction".

It is clear that we shall also investigate, when possible, their local and global stability, both via the support of the theory and some numerical tools, as already used in Figs. 1 and 2.

We can immediately see that the coordinate axes are invariant. In fact, considering a point $(x_1, 0)$ on the x_1 axis we have that $T(x_1, 0)$ belongs to the x_1 axis, and

$$T_1(x_1,0) = \begin{cases} 0 & \text{if } F_1(x_1,0) \le 0 \\ F_1(x_1,0) & \text{if } 0 \le F_1(x_1,0) \le N_1 \\ N_1 & \text{if } F_1(x_1,0) \ge N_1 \end{cases} \tag{13}$$

where

$$F_1(x_1,0) = x_1\left[1+\gamma x_1\tau_1\left(1-\frac{x_1}{N_1}\right)\right]. \tag{14}$$

Considering the restriction $t_1(x_1) \equiv T_1(x_1, 0)$ we have that $t_1(x_1) = x_1$ is satisfied for $x_1^* = 0$ (representing the origin O of T), and $x_1^* = N_1$ which represents the fixed point

$$Q_1 = (N_1, 0) \tag{15}$$

of T belonging to the x_1 axis and corner point of the range D. Regarding its local stability, since $F_1(x_1, 0) = N_1$ for $x_1 = N_1$ and $x_1 = \sqrt{\frac{N_1}{\gamma\tau_1}}$, satisfying $\sqrt{\frac{N_1}{\gamma\tau_1}} < N_1$ for $\gamma N_1\tau_1 > 1$, we have that on the right side of $x_1^* = N_1$ the map t_1 is smooth when $\gamma N_1\tau_1 > 1$ and constant otherwise, while on its left side the map is either constant (when $\gamma N_1\tau_1 > 1$) or smooth. Moreover, from $\frac{d}{dx_1}t_1(x_1) = 1 + 2\gamma\tau_1 x_1 - 3\frac{\gamma\tau_1}{N_1}x_1^2$ we have $\frac{d}{dx_1}t_1(N_1) = 1 - \gamma\tau_1 N_1 < 1$ so that this fixed point is attracting on its left side, since for $\gamma\tau_1 N_1 < 1$ it is also $\frac{d}{dx_1}t_1(N_1) > -1$.

It is worth noting that for the two-dimensional map T this fixed point is a corner point of D, so that its local dynamic behavior outside the invariant axis depends on the behaviors in the other regions Ω_5 and Ω_1 belonging to its neighborhood, and we shall return to this fixed point later. While considering the origin we have $\frac{d}{dx_1}t_1(0) = 1$ and $\frac{d^2}{d^2x_1}t_1(x_1) = 2\gamma\tau_1 - 6\frac{\gamma\tau_1}{N_1}x_1$ leads to $\frac{d^2}{d^2x_1}t_1(0) = 2\gamma_1\tau_1 > 0$ so that the fixed point $x_1^* = 0$ is repelling on its right side, that is, the origin $(0, 0)$ is repelling along the x_1 direction.

For the second axis we have $T(0, x_2) = (0, T_2(0, x_2))$ where

$$T_2(0,x_2) = \begin{cases} 0 & \text{if } F_2(0,x_2) \le 0 \\ F_2(0,x_2) & \text{if } 0 \le F_2(0,x_2) \le K_2 \\ K_2 & \text{if } F_2(0,x_2) \ge K_2 \end{cases} \tag{16}$$

and

$$F_2(0,x_2) = x_2[1+\gamma\tau_2(N_2 - x_2)]. \tag{17}$$

Considering the restriction $t_2(x_2) \equiv T_2(0, x_2)$ it follows that $x_2^* = 0$ is a fixed point of t_2 (representing the origin O of T), and since $K_2 \le N_2$ also $x_2^* = K_2$ is another fixed point of the restriction $t_2(x_2)$ on the x_2-axis, so that

$$Q_2 = (0, K_2) \tag{18}$$

is a fixed point of T. Concerning the stability of these fixed points of $t_2(x_2)$, from $\frac{d}{dx_2}t_2(x_2) = 1 + \gamma\tau_2(N_2 - 2x_2)$ we have $\frac{d}{dx_2}t_2(0) = 1 + \gamma\tau_2 N_2 > 1$ so that $x_2 = 0$ is repelling for t_2 (and thus the origin $(0, 0)$ is repelling for T). While regarding the other fixed point $x_2^* = K_2$, it is superstable for the restriction when $K_2 < N_2$. For $K_2 = N_2$ we have $\frac{d}{dx_2}t_2(N_2) = 1 - \gamma\tau_2 N_2 < 1$ so that as long as $\gamma\tau_2 N_2 < 1$ holds, leading to $\frac{d}{dx_2}t_2(N_2) > -1$, this fixed point attracts the points smaller than x_2^* on the border of D.

As a fixed point of T, we notice that also Q_2 is a border point of D. The curve $BC_{2,0}$ intersects the x_2-axis in the point $(0, 1/\gamma)$ and assuming $K_2 \le N_2 \le 1/\gamma$ the region Ω_4 does not intersect D.

For $K_2 < N_2$ the fixed point Q_2 is internal to the region $\Omega_9 \cap D$, while for $K_2 = N_2$ it is on the border of region Ω_9. Thus, for $K_2 < N_2$ the fixed point Q_2 is also a fixed point of the map on the straight line $x_2 = K_2$ defined as

$$x_1' = x_1\left[1 - \gamma K_2 + \gamma x_1\tau_1\left(1-\frac{x_1}{N_1}\right)\right] \tag{19}$$

whose derivative in $x_1 = 0$ (corresponding to Q_2) is given by $(1 - \gamma K_2) < 1$ and it is attracting when the derivative is positive, $(1 - \gamma K_2) > 0$ for $K_2 \le \frac{1}{\gamma}$. However, also $(1 - \gamma K_2) < 0$ leads to stability because by definition of map T, the constraint brings the iterated point on the axis $x_1 = 0$.

So the segregation equilibria always exist. At $Q_1 = (N_1, 0)$ the local population survives and newcomers' population exits the district definitely, at $Q_2 = (0, K_2)$ newcomers' population survives and the local population exits the district definitely. Also $O = (0, 0)$ is an equilibrium (at which both populations exit the district definitely), and as remarked above, it is a locally repelling fixed point of T. However, by definition all the points of the region Ω_3 are mapped into the origin, and when Ω_3 has a portion in D then we have a typical case of overshooting. That is, there exists a positive set of points in D and outside a small neighborhood of O, which taken as initial conditions (i.c. henceforth for short) lead to the exit of both populations. This occurs when the parameters are such that $F_1(N_1, K_2) < 0$ and $F_2(N_1, K_2) < 0$ which are satisfied for

$$\begin{aligned} &1 - \gamma K_2 < 0 \\ &1 + \gamma K_2 \tau_2 (N_2 - K_2) - \gamma N_1 < 0. \end{aligned} \tag{20}$$

Regarding the fixed points on the axes we can therefore state the following:

Proposition 2. *The map T can have the following fixed points on the coordinate axes:*

- $Q_1 = (N_1, 0)$ *always exists and it can be either locally stable or locally unstable. It is stable when* $\tau_1 < \frac{2}{\gamma N_1}$ *and unstable otherwise;*
- $Q_2 = (0, K_2)$ *always exists and it is stable for* $K_2 < N_2$;
- $O = (0, 0)$ *always exists and it is locally unstable, but it has a basin of attraction of positive measure in D when* $\Omega_3 \cap D \neq \varnothing$.

Concerning the internal fixed points, they may exist belonging to region Ω_1 given by the solutions of:

$$\begin{cases} x_1 R_1(x_1) = x_2 \\ x_2 R_2(x_2) = x_1 \end{cases} \tag{21}$$

when admissible (i.e. belonging to region $\Omega_1 \cap D$). In the phase plane these points belong to the intersection of the two reaction curves:

$$\phi_1 : x_2 = x_1 R_1(x_1), \quad \phi_2 : x_1 = x_2 R_2(x_2) \tag{22}$$

that is:

$$\begin{aligned} &\phi_1 : x_2 = x_1 \tau_1 \left(1 - \frac{x_1}{N_1}\right) \\ &\phi_2 : x_1 = \tau_2 (N_2 - x_2) \end{aligned} \tag{23}$$

whose solutions must satisfy the following equation:

$$x_1^2 - N_1 \left(1 + \frac{1}{\tau_1 \tau_2}\right) x_1 + \frac{N_1 N_2}{\tau_1} = 0 \tag{24}$$

leading to two possible fixed points of non-segregation

$$P_- = \left(x_{1-}^*, x_{2-}^*\right), \quad P_+ = \left(x_{1+}^*, x_{2+}^*\right) \tag{25}$$

where

$$\begin{aligned} x_{1\pm}^* &= N_1 \frac{\tau_1 \tau_2 + 1}{2\tau_1 \tau_2} \pm \sqrt{\left(N_1 \frac{\tau_1 \tau_2 + 1}{2\tau_1 \tau_2}\right)^2 - \frac{N_1 N_2}{\tau_1}} \\ x_{2\pm}^* &= N_2 - \frac{x_{1\pm}^*}{\tau_2} = N_2 - N_1 \frac{\tau_1 \tau_2 + 1}{2\tau_1 \tau_2^2} \\ &\quad \mp \frac{1}{\tau_2} \sqrt{\left(N_1 \frac{\tau_1 \tau_2 + 1}{2\tau_1 \tau_2}\right)^2 - \frac{N_1 N_2}{\tau_1}} \end{aligned} \tag{26}$$

with $x_{1-}^* < x_{1+}^*$. This pair of real solutions exists for $\frac{1}{\tau_2} > \sqrt{\frac{4N_2\tau_1}{N_1}} - \tau_1$, which is satisfied obviously for $\frac{4N_2}{N_1} < \tau_1$, or, more generally, it is satisfied when

$$\tau_2 < \tau_2^{SN}, \quad \tau_2^{SN} = \frac{1}{\sqrt{\frac{4N_2\tau_1}{N_1}} - \tau_1}. \tag{27}$$

We have so proved the following:

Proposition 3. *At* $\tau_2 = \tau_2^{SN}$, *that is,*

$$(SN): \quad \tau_2 = \frac{1}{\sqrt{\frac{4N_2\tau_1}{N_1}} - \tau_1} \tag{28}$$

a saddle-node bifurcation occurs and the two merging fixed points $P_- = P_+ = \left(x_1^*, x_2^*\right)$ *have coordinates given by*

$$x_1^* = \frac{N_1}{2}\left(1 + \frac{1}{\tau_1 \tau_2}\right), \quad x_2^* = N_2 - \frac{x_1^*}{\tau_2} \tag{29}$$

and a pair of natural fixed points of non-segregation $P_- = \left(x_{1-}^*, x_{2-}^*\right)$ *and* $P_+ = \left(x_{1+}^*, x_{2+}^*\right)$ *exist for* $\tau_2 < \tau_2^{SN}$, *given in (26), which are real for T when belonging to the region* $\Omega_1 \cap D$.

In Fig. 3 are shown a few examples of the bifurcation curves $\tau_2 = \tau_2^{SN}$ associated with the appearance/disappearance of the pair of fixed points of non-segregation P_- and P_+. These fixed points can be either a saddle and an attracting node or a saddle and a repelling node, and both cases may occur in the phase space of interest for us. It is worth noting that the coordinates of the fixed points of non-segregation P_- and P_+ are independent of the value of γ. However, their local stability is influenced by γ.

For the complete understanding of the real existence of the natural fixed points of non-segregation we have to show that after the occurrence of the saddle-node bifurcation ($\tau_2 < \tau_2^{SN}$ as shown above) they do not become virtual, which can occur both via a border collision due to the merging with the fixed point Q_1 and via a border collision with the upper boundary of D. This is associated with the appearance of the other fixed points introduced above, the artificial fixed points of non-segregation, that we are going to determine below.

To this purpose, let us notice that the reaction curve ϕ_2 is the straight line $x_1 = \tau_2(N_2 - x_2)$ while the reaction curve ϕ_1 is a concave parabola always crossing through the points O and Q_1. Moreover, it can be seen that the three curves ϕ_1, BC_1 and $x_1 = N_1$ (boundary of D) all intersect at the fixed point Q_1. Similarly, the three curves ϕ_2, BC_2 and $x_2 = K_2$ (boundary of D) all intersect at the point Q given by:

$$Q = (x_{1,m}, K_2), \quad x_{1,m} = \tau_2(N_2 - K_2) \tag{30}$$

(see the point Q in Figs. 1 and 2). In fact, $x_2 = K_2$ intersects BC_2 (of equation $x_1 = \frac{1}{\gamma} + \tau_2(N_2 - x_2) - \frac{K_2}{\gamma x_2}$) at the point $x_{1,m} = \tau_2(N_2 - K_2)$, and also $x_2 = K_2$ intersects ϕ_2 (of equation $x_1 = \tau_2(N_2 - x_2)$) at the same point. For $K_2 = N_2$ we have $Q = Q_2$ while when $K_2 < N_2$ the point Q is on the upper boundary of D and $\Omega_9 \cap D \neq \varnothing$, as in the example shown in Fig. 1a.

The above observation leads to determine the artificial fixed points of non-segregation which may occur only when $K_2 < N_2$, when there is a portion $\Omega_9 \cap D$ which is mapped into the line $x_2 = K_2$, where the map is given in (19) for

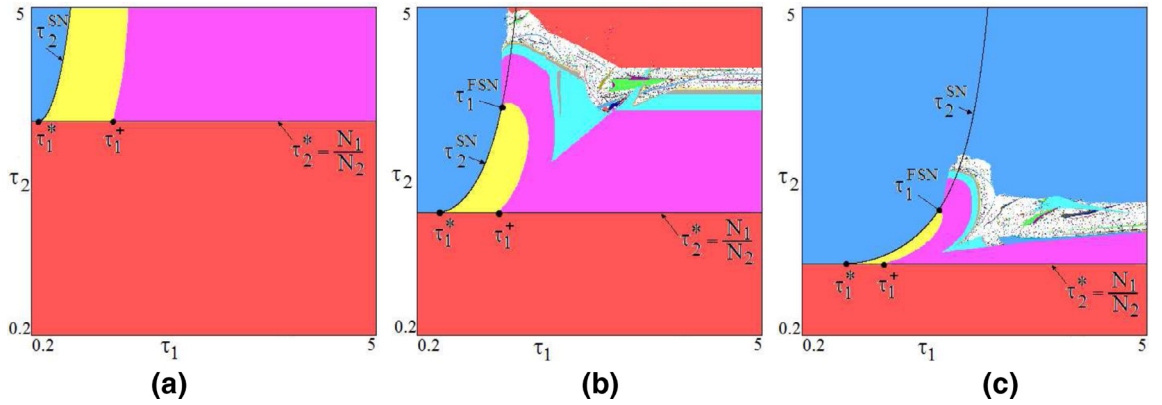

Fig. 3. Two-dimensional bifurcation diagram in the parameter plane (τ_1, τ_2) at $\gamma = 1.5$ for different values of N_2 and no entry constraints, i.e. $K_2 = N_2$. Panel (a), $N_2 = 0.3$, Panel (b), $N_2 = 0.5$, Panel (c), $N_2 = 0.8$. The red region represents the set of values of (τ_1, τ_2) for which the equilibrium Q_1 has a basin of attraction of positive measure in D. The azure region indicates that the only stable fixed point of map T is Q_2. For points in the yellow region the equilibrium P_+ is stable. The magenta region corresponds to a stable 2-cycle. Other colors represent stable cycles of higher periods and the white region indicates the presence of a chaotic attractor. (For interpretation of the references to color in this figure legend, the reader is referred to the web version of this article.)

$0 \le x_1 < x_{1,m}$ and in this case other possible constrained fixed points are those obtained as intersection of the line $x_2 = K_2$ with the reaction curve ϕ_1, when belonging to region Ω_9. So let us determine the solutions of $K_2 = x_1\tau_1(1 - \frac{x_1}{N_1})$ obtaining

$$\bar{x}_{1\pm} = \frac{N_1}{2} \pm \sqrt{\left(\frac{N_1}{2}\right)^2 - \frac{N_1 K_2}{\tau_1}} \tag{31}$$

leading to two possible fixed points:

$$\bar{P}_- = (\bar{x}_{1-}, K_2), \quad \bar{P}_+ = (\bar{x}_{1+}, K_2). \tag{32}$$

As already noticed, the natural fixed points of non-segregation P_- and P_+ exist when they belong to the proper region Ω_1, otherwise a fixed point is called virtual (i.e. it is not a true fixed point for the map), and by their definition the fixed points P_- and P_+ can become virtual colliding (in a border collision) with the fixed point Q_1 or colliding with the upper boundary of D in the point Q.

From the expressions of the coordinates of the fixed points we have that for $x_{1,m} = \tau_2(N_2 - K_2) < x^*_{1-} < x^*_{1+} < N_1$ both the natural fixed points of non-segregation P_- and P_+ exist inside the region $\Omega_1 \cap D$.

Then a border collision occurs when there is the merging $P_+ = Q_1$. This leads to the conditions $x^*_{1+} = N_1$ and $x^*_{2+} = 0$, from which (by using $x^*_{2+} = N_2 - \frac{x^*_{1+}}{\tau_2} = 0$) it is immediate to get $\tau_2 = \frac{N_1}{N_2}$.

Moreover, considering that the saddle-node bifurcation occurs at $\tau_2 = \tau_2^{SN}$, we have that at the intersection point of the two curves (saddle node $\tau_2 = \tau_2^{SN}$ and border collision) the merging $P_- = P_+ = Q_1$ occurs. By using the expression in (28) and $\tau_2 = \frac{N_1}{N_2}$ we obtain that this occurs at $\tau_1 = \frac{N_2}{N_1}$. We have so proved the following:

Proposition 4. *The border collision bifurcation at which P_+ collides with Q_1 takes place for*

$$\tau_2 = \tau_2^* \quad \text{and} \quad \tau_1 > \tau_1^* \tag{33}$$

where

$$\tau_2^* = \frac{N_1}{N_2}, \quad \tau_1^* = \frac{1}{\tau_2^*} = \frac{N_2}{N_1}. \tag{34}$$

The bifurcation point (τ_1^*, τ_2^*) is a codimension-two point at which the saddle node and the border collision occur simultaneously:$P_- = P_+ = Q_1$.

The other possible border collisions occur when the natural fixed points of non-segregation P_- and P_+ collide with the border point Q. That is:

- a border collision due to the merging $P_- = Q$ leads to the disappearance of P_- and appearance of the artificial fixed point of non-segregation $\bar{P}_-$;
- a border collision due to the merging $P_+ = Q$ leads to the disappearance of P_+ and appearance of the artificial fixed point of non-segregation $\bar{P}_+$.

Considering the coordinates of the fixed points then

- when $x_{1,m} = \tau_2(N_2 - K_2) = x^*_{1-}$ a border collision occurs due to the merging $P_- = Q$;
- when $x_{1,m} = \tau_2(N_2 - K_2) = x^*_{1+}$ a border collision occurs due to the merging $P_+ = Q$;

so that we have the following:

Proposition 5. *The border collision at which P_- merges with Q takes place for $x_{1,m} = x^*_{1-}$ and $K_2 = x^*_{2-}$, leading to the following bifurcation condition:*

$$\tau_2(N_2 - K_2) = N_1\frac{\tau_1\tau_2 + 1}{2\tau_1\tau_2} - \sqrt{\left(N_1\frac{\tau_1\tau_2 + 1}{2\tau_1\tau_2}\right)^2 - \frac{N_1N_2}{\tau_1}}. \tag{35}$$

The border collision at which P_+ merges with Q occurs for $x_{1,m} = x^*_{1+}$ and $K_2 = x^*_{2+}$, leading to the following bifurcation condition:

$$\tau_2(N_2 - K_2) = N_1\frac{\tau_1\tau_2 + 1}{2\tau_1\tau_2} + \sqrt{\left(N_1\frac{\tau_1\tau_2 + 1}{2\tau_1\tau_2}\right)^2 - \frac{N_1N_2}{\tau_1}}. \tag{36}$$

Summarizing, we have that the possible occurrences for the natural and artificial fixed points of non-segregation are as described in the following:

Proposition 6. *Concerning the fixed points of non-segregation, the following cases are possible:*

(i) *let* $x_{1,m} = \tau_2(N_2 - K_2) < x^*_{1-} < x^*_{1+} < N_1$, *then both the natural fixed points of non-segregation* P_- *and* P_+ *exist inside the region* $\Omega_1 \cap D$;
(ii) *let* $x_{1,m} = \tau_2(N_2 - K_2) < x^*_{1-} < N_1 < x^*_{1+}$, *then only* P_- *is inside the region* $\Omega_1 \cap D$ *while* P_+ *is virtual, and this can occur "after" the collision of* P_+ *with* Q_1;
(iii) *let* $\tau_2 = \tau_2^*$ *and* $\tau_1 = \tau_1^*$, *then* $P_+ = P_- = Q_1$, *and this corresponds to a codimension-two bifurcation as both the saddle-node* $\tau_2 = \tau_2^{SN}$ *and the border collision with* Q_1, $x^*_{2-} = x^*_{2+} = 0$ *and* $x^*_{1-} = x^*_{1+} = N_1$ *occur;*
(iv) *let* $x_{1,m} = \tau_2(N_2 - K_2) < N_1 < x^*_{1-} < x^*_{1+}$, *then both* P_+ *and* P_- *are virtual, outside region* D;
(v) *let* $x^*_{1-} < x_{1,m} < x^*_{1+} < N_1$, *then only* P_+ *is in region* $\Omega_1 \cap D$ *while* P_- *no longer exists (becomes virtual), and there is the artificial fixed point of non-segregation* $\overline{P}_- = (\overline{x}_{1-}, K_2)$;
(vi) *let* $x^*_{1-} < x^*_{1+} < x_{1,m} < N_1$ *then both* P_- *and* P_+ *are virtual while both the artificial fixed points of non-segregation* $\overline{P}_-$ *and* $\overline{P}_+$ *exist.*

Regarding the stability of the natural fixed points of non-segregation P_- and P_+ when they belong to the region $\Omega_1 \cap D$ in which the map is smooth, by simple considerations we can conclude that P_- is crossed by at least an unstable manifold while P_+ is crossed by at least a stable manifold. Indeed, inside the region $\left\{(x_1, x_2) | x_1 \in \left(x^*_{1-}, x^*_{1+}\right) \text{ and } x_2 < x_1 R(x_1)\right\}$ that join P_- and P_+ (see Fig. 1a) it is such that $F_1(x_1, x_2) > 0$ and hence the state variable x_1 moves from x^*_{1-} towards x^*_{1+}. Moreover, we can investigate the local stability making use of the Jacobian matrix evaluated at an equilibrium point $P = \left(x^*_1, x^*_2\right)$ not belonging to the boundary of D given by

$$J(x^*_1, x^*_2) = \begin{bmatrix} 1 + \gamma\tau_1 x^*_1\left(1 - 2\frac{x^*_1}{N_1}\right) & -\gamma x^*_1 \\ -\gamma x^*_2 & 1 - \gamma\tau_2 x^*_2 \end{bmatrix} \tag{37}$$

and the characteristic polynomial takes the form

$$\rho(\lambda) = \lambda^2 - T_r\lambda + \det \tag{38}$$

with

$$T_r = \lambda_1 + \lambda_2 = 2 + \gamma\tau_1 x^*_1\left(1 - 2\frac{x^*_1}{N_1}\right) - \gamma\tau_2 x^*_2$$

$$\det = \lambda_1\lambda_2 = \left(1 + \gamma\tau_1 x^*_1\left(1 - 2\frac{x^*_1}{N_1}\right)\right)(1 - \gamma\tau_2 x^*_2) - \gamma^2 x^*_1 x^*_2 \tag{39}$$

where $\lambda_{1,2}$ are the roots of the characteristic equation $\rho(\lambda) = 0$.

By the local analysis, via the eigenvalues, when the fixed point P_+ merges with Q_1 it can be either a stable node or a saddle. As P_- is necessarily unstable, the fixed point P_+ can be locally attracting and may become unstable via a flip bifurcation when $\rho(-1) = 0$. The appearance of a stable 2-cycle when one eigenvalue related to $J(P_+)$ crosses -1 has been observed numerically.

We can summarize the results associated with the local stability of the fixed points in the following:

Proposition 7. *The map T can have the following fixed points:*

- $P_- = (x^*_{1-}, x^*_{2-})$ *, if it exists then it can be either a saddle or an unstable node;*
- $P_+ = (x^*_{1+}, x^*_{2+})$ *, if it exists then it can be either a stable node or a saddle;*
- $\overline{P}_- = (x^+_{1-}, K_2)$ *, if it exists then it can be either a saddle or a repelling node;*
- $\overline{P}_+ = (x^+_{1+}, K_2)$ *, if it exists then it can be either a stable fixed point or a saddle.*

3.1. Codimension-two bifurcation points

We have remarked above the occurrence of a codimension-two bifurcation point, (τ_1^*, τ_2^*), at which $P_+ = P_- = Q_1$, so that both the saddle-node $\tau_2 = \tau_2^{SN}$ and the border collision $\tau_2 = \tau_2^*$ take place. Other codimension-two points can be noticed in Fig. 3.

One is associated with the flip bifurcation of P_+ which can occur when the border collision $P_+ = Q_1$ takes place. This leads to the condition $1 + T_r + \det = 0$ when computed at $(x^*_1, x^*_2) = (N_2, 0)$ and it is straightforward to get the following condition:

$$\tau_2 = \tau_2^* \quad \text{and} \quad \tau_1 = \tau_1^+, \quad \text{where} \quad \tau_1^+ = \frac{2}{\gamma N_1}. \tag{40}$$

See the points (τ_1^+, τ_2^*) in Fig. 3.

In Fig. 3 we can notice one more codimension-two bifurcation point, denoted τ_2^{FSN} which is a contact point between the saddle-node curve $\tau_2 = \tau_2^{SN}$ and the flip bifurcation curve of the fixed point P_+. To determine this point let us consider that to have simultaneously a saddle-node ($P_- = P_+$) and a flip bifurcation of P_+ it is necessary to have two eigenvalues at the bifurcation value, $\lambda_1 = 1$ and $\lambda_2 = -1$. Thus from the condition $T_r = \lambda_1 + \lambda_2 = 0$ and $\tau_2 = \tau_2^{SN}$ we obtain:

$$\tau_1 = \tau_1^{FSN}, \quad \tau_1^{FSN} = \frac{\gamma N_1\left(1 + \left(\tau_2^{SN}\right)^2\right)}{\left(4\tau_2^{SN} - \gamma N_1 - \gamma N_1\left(\tau_2^{SN}\right)^2\right)\tau_2^{SN}} \tag{41}$$

and substituting τ_2^{SN} we obtain the bifurcation condition:

$$4\tau_1\sqrt{\frac{N_2\tau_1}{N_1}} - 2\tau_1^2 - 4\gamma N_2\tau_1\sqrt{\frac{N_2\tau_1}{N_1}} + 2\gamma N_2\tau_1^2 + 2\gamma N_2\tau_1^2 + \gamma\tau_1^2\sqrt{N_1N_2\tau_1} - \gamma\sqrt{N_1N_2\tau_1} = 0. \tag{42}$$

We only have numerical evidence of the dynamic result related to these bifurcations. Changing the parameters from a codimension-two bifurcation point, the results may differ, depending on the region in the parameter space in which the parameters are moved.

From the analysis performed up to now, it emerges that in the particular case without entry limitations, i.e. $K_2 = N_2$, the point P_+ can be the only stable equilibrium of non-segregation. Moreover, there is a set of values of the parameters such that the equilibrium P_+ is never feasible, given by $\tau_2 < \tau_2^*$. It means that, without entry limitations, a minimum level of tolerance from newcomers, measured by the value τ_2^*, is required to have the necessary condition for a stable equilibrium of non-segregation.

In the next sections we make use of numerical tools to describe the global dynamics of the model and to comment

it from a socioeconomic point of view, with some emphasis on the policy implications.

4. The dynamics of the model without entry limitations

As a starting point, let us analyze the dynamics of the model by means of two-dimensional (2D for short) bifurcation diagrams in the parameter plane of the two parameters of tolerance, i.e. (τ_1, τ_2), where τ_1 and τ_2 vary in the range [0.2, 5] . This range is set large enough to include almost all the bifurcations that occur as the two parameters are changed. Setting $\gamma = 1.5$, $N_1 = 1$ and $K_2 = N_2$ (i.e., no entry limitations for newcomers), the 2D bifurcation diagrams are reported in Fig. 3 for different values of the parameter N_2.

From Fig. 3 we note that for relative low values of τ_2, i.e. $\tau_2 < \tau_2^*(=\frac{N_1}{N_2})$ indicated by the red region, whatever the level of tolerance of the local population, the only stable fixed points are the segregation ones, i.e. Q_1 and Q_2. Thus, if the population of newcomers is characterized by low level of tolerance there are no possibilities to avoid segregation, at least without external restrictions to the entry and exist dynamics. The threshold level $\tau_2 = \tau_2^*(=\frac{N_1}{N_2})$ (border collision bifurcation value at which P_+ merges with Q_1) represents the minimal level of tolerance required by newcomers under which segregation occurs for sure and it is inversely related to their numerosity.

As the value of τ_2 increases, we have a transition to three possible scenarios. Which one of the three depends on the level of tolerance of the local population, i.e. on the level of τ_1. If τ_1 is small, specifically $\tau_1 < \tau_1^*(=\frac{1}{\tau_2^*}=\frac{N_2}{N_1})$, so that the local population has a very limited level of tolerance towards newcomers, increasing τ_2 we move from the red region, characterized by the two stable fixed points of segregation Q_1 and Q_2, to the blue region, characterized by Q_2 as the unique stable fixed point. Indeed, the blue region in the 2D bifurcation diagrams represents situations such that the local population is highly intolerant and is prepared to abandon its neighborhood as soon as a small number of newcomers enter the district and settle in it. At the same time, the newcomers have a high level of tolerance and so they stand the presence of the local population and enter the district. In the end, the local population can only leave the district and the fixed point of segregation Q_2 is the unique final stage of the process.

On the contrary, if the local population is partially tolerant towards the newcomers, specifically $\tau_1^* < \tau_1 < \tau_1^+(=\frac{2}{\gamma N_1})$, then as τ_2 increases from τ_2^* we experience a transition from a region of segregation, the red region, to a region of non-segregation, the yellow region (see Fig. 3). The yellow region is the only region of the entire parameter space in which the entry-exit dynamics of the segregation model is able to self-converge to a stable equilibrium of non-segregation. This region indicates a situation for which both the local population and the population of newcomers have neither a too low level of tolerance that would prevent the coexistence nor a too high level of tolerance that is responsible for entry/exit overreactions by the members of the two populations that threaten the coexistence.

It is worth noticing that by increasing further the level of tolerance of the newcomers, the natural fixed point of non-segregation P_+ can either disappear through a saddle-node bifurcation (from the yellow region to the blue region crossing the saddle-node bifurcation curve $\tau_2 = \tau_2^{SN}$), or P_+ can become unstable via a flip bifurcation leading to a stable 2-cycle (from the yellow region to the magenta region crossing the flip bifurcation curve $\rho(-1) = 0$).

From the magenta region, a further increase of the level of tolerance of the newcomers produces a sequence of period doubling bifurcations after which a two-piece chaotic attractor is observable. This route can be seen in the one-dimensional (1D for short) bifurcation diagram of Fig. 4c along the path marked by a vertical segment and an arrow in Fig. 4a. The two disjoint chaotic sets are two separate chaotic attractors for the second iterate of the map, i.e. map T^2, each with its own basin of attraction, as shown in Fig. 4d by the white region and the red region. The structure of the two basins of attraction of Fig. 4d indicates the presence of a fractal frontier which includes a chaotic repellor. It is worth noting that this chaotic repellor on the frontier of the basins of T^2 is not related to the forward sequence of bifurcations leading to the chaotic sets. Instead, it is related to a sequence of period doubling bifurcations of unstable cycles that starts from the fixed point of non-segregation P_-. That is the saddle fixed point P_- becomes a repelling node leading to a saddle 2-cycle on the frontier of $\mathcal{B}(Q_2)$ the basin basin of attraction of Q_2. The saddle 2-cycle becomes a repelling node leading to a saddle 4-cycle on the same frontier, and so on, leading to a chaotic repellor on the frontier of $\mathcal{B}(Q_2)$.

It is worth noting that at the values of the parameters considered in Fig. 4d the two disjoint chaotic sets are very close to the boundary of their basins and a slight increase in τ_2 leads to the disappearance of the chaotic attractor. After such a contact almost all the points in the phase space have a trajectory which is convergent to Q_2. However a chaotic repellor persists (consisting of all the unstable cycles existing in the chaotic region of Fig. 4d), and this leads to the phenomenon of chaotic transient, which can be also very long, before the convergence to Q_2. An example is shown in Fig. 4b, where a unique trajectory of T shows the " ghost" of the old attractor clearly visible for a large number of iterations before converging to Q_2, and also persists for a set of values of τ_1 and τ_2.

Of particular interest is also the bifurcation that occurs when increasing τ_2 we move from the white region of the 2D parameter space of Fig. 3b to the upper red region. In the white region the fixed point of segregation Q_1 is locally unstable but not globally in D and a chaotic attractor exists, as shown in Fig. 5a. Starting from this situation and increasing τ_2 in such a way as to move from the red region to the white region, the chaotic attractor disappears through a border collision with the border $x_2 = 0$ of D. As we know, all trajectories in $x_2 = 0$ of D (excluding the origin O) converge to Q_1, thus after the contact we observe that the basin of attraction of Q_1 becomes a large part of D, as shown in Fig. 5b, including the unstable manifold of Q_1 given by $x_1 = 1$. So, also a trajectory that starts on the unstable manifold converges in the end to Q_1.

This contact bifurcation (also known as "final bifurcation" of the internal attractor) represents a phenomenon of overshooting. This dynamic scenarios underlines that an excess of the level of tolerance by newcomers could be harmful and

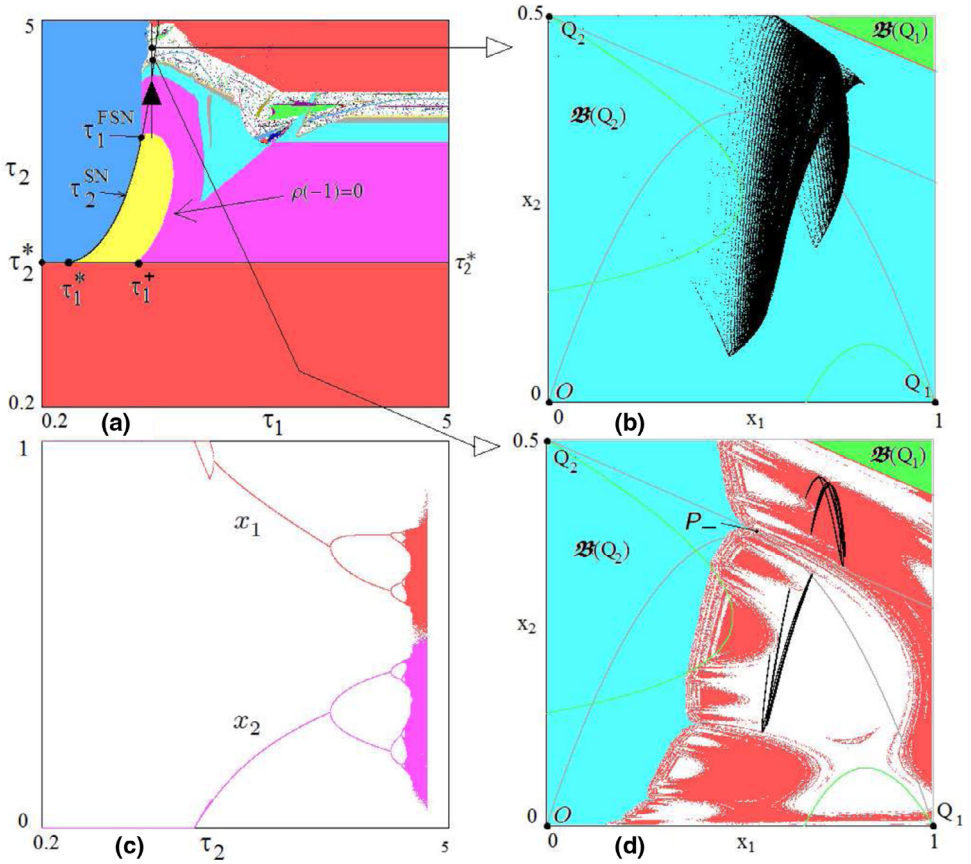

Fig. 4. Panel (a): 2D bifurcation diagram as in Fig. 3b. In Panel (c) the 1D-bifurcation diagrams of x_1 (in red) and x_2 (in magenta) along the vertical path marked in Panel (a) at $\tau_1 = 1.5$, $\tau_2 \in [0.2, 5]$, $N_2 = 0.5$. Panel (d), phase space D with the basins for T^2. Panel (b), "ghost attractor", or chaotic transient, after the contact of the attractor with its basin boundary. (For interpretation of the references to color in this figure legend, the reader is referred to the web version of this article.)

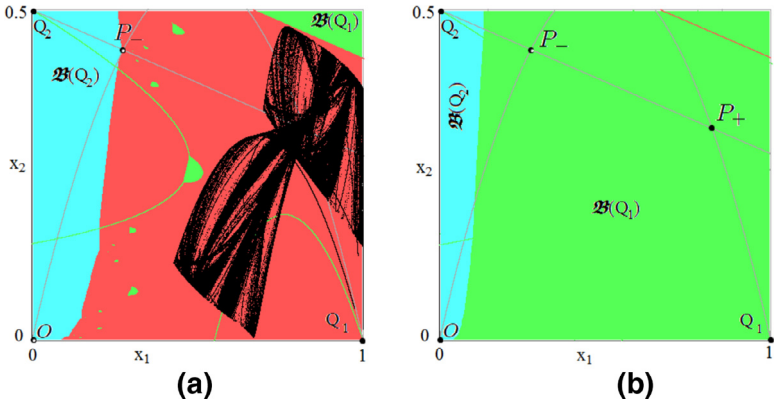

Fig. 5. Basins of attraction: Azure region is the basin of attraction of the segregation fixed point Q_2, green region is the basin of attraction of the segregation fixed point Q_1, red region is the basin of attraction of the chaotic attractor at $\tau_1 = 2.2$, $N_2 = 0.5$, $\gamma = 1.5$. Panel (a), $\tau_2 = 4.54$. Panel (b), $\tau_2 = 4.6$. (For interpretation of the references to color in this figure legend, the reader is referred to the web version of this article.)

could prevent integration between the newcomers and the local population.

The scenario is slightly different for $\tau_1 > \tau_1^+$. In fact, in this case a higher level of tolerance of the local population prevents the stability of the natural fixed point of non-segregation P_+. In particular, as the level of tolerance of the newcomers increases we have a transition from the red region, where only the two fixed points of segregation Q_1 and Q_2 are stable, to the magenta region, where a stable 2-cycle coexists with the stable fixed point of segregation Q_2.

It is worth noticing that for values of τ_1 larger than a suitable level, say $\tau_1 > \overline{\tau}_1 > \tau_1^+$, all the cycles and chaotic

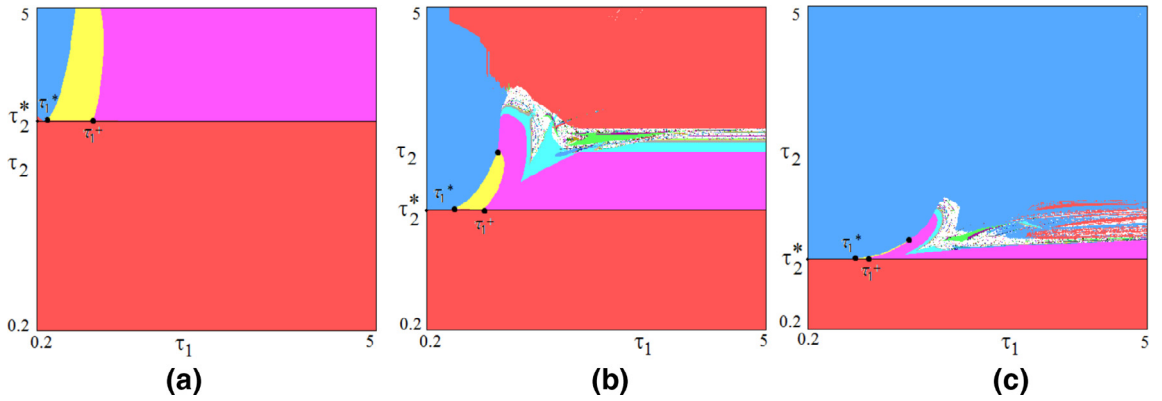

Fig. 6. 2D bifurcation diagram in the (τ_1, τ_2) parameter plane at $\gamma = 2$ and no entry constraints, i.e. $K_2 = N_2$, for different values of N_2: Panel (a), $N_2 = 0.3$, Panel (b), $N_2 = 0.5$, Panel (c), $N_2 = 0.8$. The red region represents the set of parameters at which the fixed point of segregation Q_1 has a basin of attraction of positive measure. The azure region indicates that the only stable fixed point of map T is the fixed point of segregation $Q_2 = (0, K_2)$. The yellow region represents the set of values for which equilibrium $P_+ = \left(x^*_{1,+}, x^*_{2,+}\right)$ is stable. The magenta one represents the region of a stable 2-cycle. Other colors represent stable cycles of higher periods and white region indicates the presence of a chaotic attractor. (For interpretation of the references to color in this figure legend, the reader is referred to the web version of this article.)

attractors that appear increasing τ_2 have at least one point in the region Ω_5 and so at least one point on the border of the region D, $x_1 = N_1$ (that is to say: the attracting sets involve some points of the boundary of D due to some border collision bifurcation).

The dynamical scenario described so far occurs for all the values of N_2 indicated in Fig. 3, i.e. $N_2 = 0.3$ (in this case to observe all the transition to chaotic attractors up to the final bifurcation it is necessary to plot the 2D parameter space for $\tau_2 > 5$), $N_2 = 0.5$ and $N_2 = 0.8$. However, it is possible to note some differences. As N_2 increases the yellow and magenta regions decrease, indicating that the stability of the natural fixed point of non-segregation and of the 2-period cycle becomes more sensitive to the tolerance parameters τ_1 and τ_2 when the population of newcomers increases. This is plausible noting that the level of tolerance of the newcomers increases also with their numerosity and we already observed that for large values of tolerance the overshooting problems occur. At the same time, the blue region increases and with it the risk of segregation.

Interestingly, increasing N_2 the chaotic region (white one) and the region with cycles of high periods increase in size. We can conclude that as the number of newcomers increases, the dynamics become more sensitive to the values of the parameters of tolerance, and the regions, for which an attractor of non-segregation exists, reduce in size, decreasing the possibility of avoiding segregation.

One more remark on this first case is shown in Fig. 3: The dynamics is more sensitive to the level of tolerance of the newcomers than to the level of tolerance of the local population. In fact, whatever is the level of tolerance of the local population we have segregation if the level of tolerance of the newcomers is not high enough, i.e. if $\tau_2 < \tau_2^*$, which can be called the region of "intolerance" of the parameter space (τ_1, τ_2), since in this region the limited level of tolerance of the two populations prevents the coexistence in the district of the two populations and only segregation is possible.

Moreover, for high levels of tolerance of newcomers the overshooting always occurs and leads to segregation,

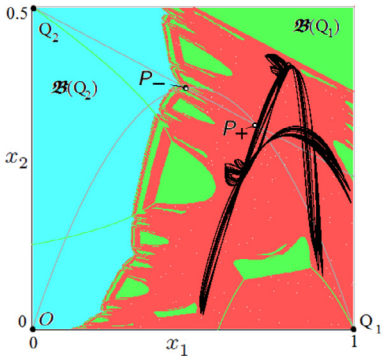

Fig. 7. Parameters: $\tau_1 = 1.5$, $\tau_2 = 3.8$, $N_2 = 0.5$, $\gamma = 2$. Chaotic attractor and basins of attraction: In azure is the basin of attraction of the segregation fixed point $Q_1 = (0, N_2)$, in red is the basin of attraction of the chaotic attractor and in green is the basin of attraction of the segregation fixed point $Q_2 = (N_1, 0)$. (For interpretation of the references to colour in this figure legend, the reader is referred to the web version of this article.)

indicating that entry limitations are necessary in this case to curb the massive entry-exit dynamics which generates overshooting and prevent the coexistence. This policy will be analyzed in more detail in the next section.

The dynamic framework here presented is quite rich and complicated. Nevertheless, it describes most of the possible dynamics that can occur with few exceptions documented in the following. In particular, similar scenarios occur for larger values of the adjustment parameter γ, see Fig. 6 for $\gamma = 2$. However, for $\gamma = 2$ it is possible to observe a 2-pieces chaotic attractor for the map T, in which a contact bifurcation leads to a one-piece chaotic attractor (merging bifurcation). See the example in Fig. 7, and compare with Fig. 4b,c. The fact that in Fig. 7 the chaotic attractor persists after the contact bifurcation in a unique chaotic set and does not disappear is due to the presence of the two internal fixed points of non-segregation P_- and P_+. Indeed, although they are unstable, their presence influences the global dynamics of the model.

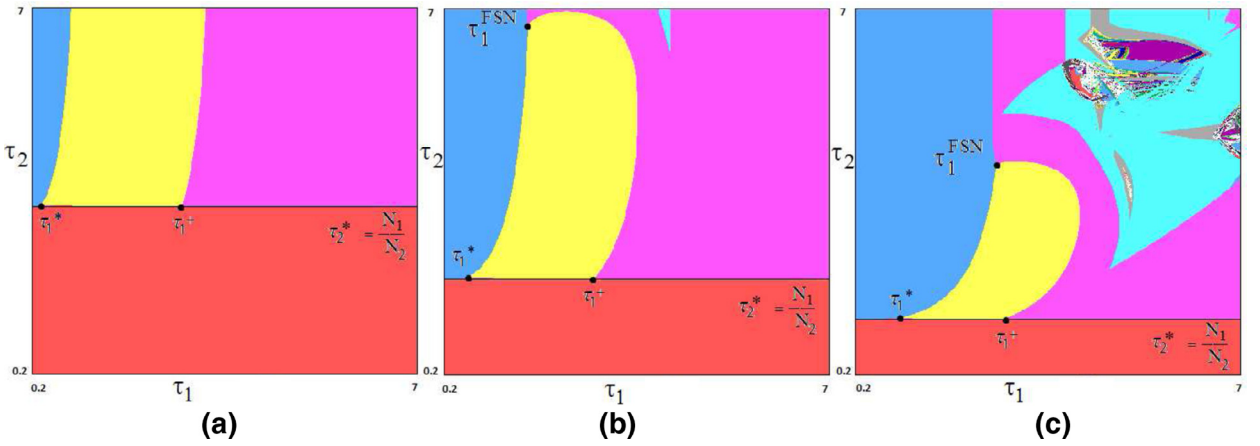

Fig. 8. 2D bifurcation diagram in the (τ_1, τ_2) parameter plane at $\gamma = 0.7$ and no entry constraints, i.e. $K_2 = N_2$, for different values of N_2. Panel (a), $N_2 = 0.3$, Panel (b), $N_2 = 0.5$, Panel (c), $N_2 = 0.8$. The meaning of the colors is the same as in Fig. 6. (For interpretation of the references to color in this figure legend, the reader is referred to the web version of this article.)

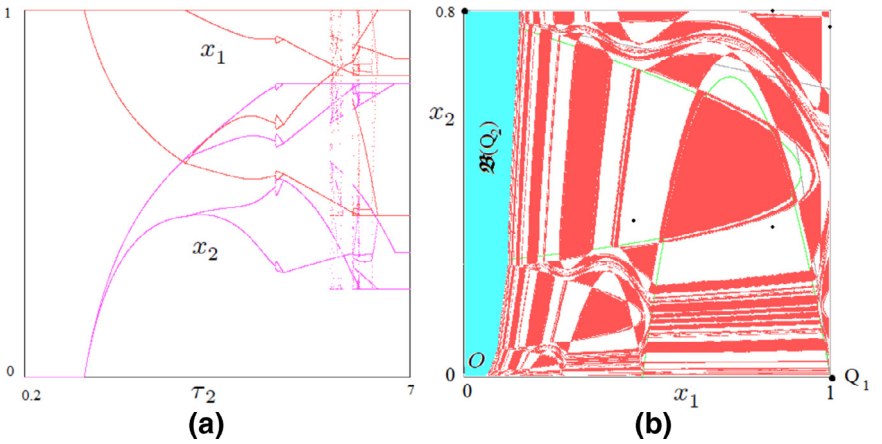

Fig. 9. Panel (a) 1D bifurcation diagram at $\tau_1 = 6$, $\tau_2 \in (0.2, 7)$, $\gamma = 0.7$, $N_2 = 0.8$. Panel (b), phase plane $D = [0, 1] \times [0, 0.8]$ at $\tau_2 = 5.8$ and basins of attraction: The azure region is the basin of attraction of the segregation fixed point $Q_1 = (0, N_2)$, the red region is the basin of attraction of the stable 6-cycle and the white region the basin of attraction of the stable 4-cycle. (For interpretation of the references to color in this figure legend, the reader is referred to the web version of this article.)

Despite the global bifurcation that is noteworthy, the numerical investigation conducted did not underline any substantial difference in the dynamics of the model of segregation for the different parameter sets used in Fig. 6.

For the sake of completeness, it is worth considering a numerical investigation for low values of the adjustment coefficient γ. Indeed, the particular economic conditions of some national economies, as it can be a quite stuck real estate market and an inflexible labor market, may imply values of the adjustment coefficient γ less than the unity. Let us choose $\gamma = 0.7$ as a representative value.[2] Comparing the case $\gamma = 0.7$ with the cases $\gamma > 1$ considered above, we note that the dynamic scenarios are not dissimilar at least for low levels of τ_2.

Looking at Figs. 8 and 3 it is possible to note an increase of the yellow region and a decrease of the size of the blue region when γ is equal to 0.7. This can be explained observing that a lower level of γ reduces the overreaction or overshooting issues. Despite the many similarities, a substantial difference observable for low level of γ is related to the white region, indicating the existence of chaotic or high-periodic attractors, which disappears for $N_2 = 0.5$ and it is observable with limited extension only for $N_2 = 0.8$. Notwithstanding the reduction of the chaotic region in the parameter plane, the dynamic scenarios in the phase space are quite complicated even for $\gamma < 1$. Indeed, for $\gamma = 0.7$ we observe the coexistence of cycles of different periods, as depicted in Fig. 9, where a stable 4-cycle coexists with a stable 6-cycle.

As a final remark on the global properties of the model, let us underline that for high levels of the adjustment coefficient the dynamics of the model can be characterized by cycles of high periods or be chaotic at least for a quite large range of values of (τ_1, τ_2). For low levels of the adjustment

[2] Other choices of the value of γ in (0, 1) would lead to similar conclusions.

parameter the cycles or chaotic attractors are less frequent. Nevertheless, other forms of complexity occur, such as the coexistence of attracting cycles and quite complicated structures of the related basins of attraction that indicate high dependence on the initial conditions (similar to what occurs in presence of chaos).

The analysis conducted reveals that the dynamics of the model is consistent with the results on segregation obtained using an agent-based approach, see e.g. [7,8] and [9]. For example the analysis conducted in [8] underlines that the level of segregation depends on two main parameters, the level of tolerance and the number of agents in the neighborhood and concludes that for low levels of tolerance the probability of having segregation is almost one while as the level of tolerance increases the risk of segregation disappears. These results are consistent with the dynamical scenarios unveiled by the 2D bifurcation diagrams indicating that for low levels of τ_1 and τ_2, the levels of tolerance of the local population and of the newcomers respectively, segregation is the only possible equilibrium of the model, see, e.g., Figs. 3, 6 and 8. Moreover, a suitable increase of τ_1 and τ_2 reduces the risk of segregation. Another aspect underlined in [8] is the number of vacancies, which in terms of the present paper can be interpreted as the total number of the members of the two populations (the maximum number of agents that can live in the neighborhood) minus the number of agents of these two populations that are inside the district. In particular, Gauvin, Vannimenus, and Nadal [8] point out that the number of vacancies is proportional to the risk of segregation and for high level of vacancies the segregation is the only possible output. The extent to which this occurs depends on the levels of tolerance. Looking at the basins of attraction we realize that this behavior is confirmed by the analyzed model as testified by the relatively large extension of the azure region (basin of attraction of one of the segregation equilibria) for $x_1 + x_2$ small and its total absence in the opposite case, see, e.g. Figs. 2, 4d and 5a. In analogy with the results in [8], we also observe that for low levels of tolerance the segregation is the only long-term solution for whatever number of vacancies. In addition to this, the present analysis underlines that a low number of vacancies and large levels of tolerance can lead to segregation due to overshooting. Moreover, [9] provides the interesting result that segregation seems to be the only possible scenario when the sensitivity of the agents to switch to the desired output increases. In analogy with [9], we observe that an increase of the adjustment parameter γ reduces the extension of the region of the parameter space for which a stable equilibrium of non-segregation exists. Compare the yellow region in Fig. 8 for $\gamma = 0.7$ with the one in Fig. 6 for $\gamma = 2$. Moreover, the examples described in [7] underline that in some cases an increase of the level of tolerance produces the unexpected result of increasing the level of segregation. This aspect is observable also in the current model for example when an increase of the levels of tolerance causes the appearance of a basin of attraction of positive measure for one of the two segregation equilibria despite its local instability. Thus, this unexpected effect can be explained in terms of Milnor attractors appearing through global bifurcations and it is associated with dynamics of overshooting, see, e.g., the green regions in Figs. 4d, 5a,b and 7.

5. The rule of entry constraints

In this section we analyze the effect of entry constraints on the segregation dynamics. In particular, we are interested in understanding the reduction of segregation that we can have if we introduce an entry constraint for population two, i.e. $0 < K_2 < N_2$. The analysis is conducted by making use of 2D bifurcation diagrams with respect to K_2 and τ_1 and with respect to K_2 and τ_2.

Let us start by considering the role of the constraints at $\gamma = 1.5$, $N_2 = 0.5$, $\tau_2 = 3.5$ and varying K_2 in the range [0, 0.5] and τ_1 in the range [0.2, 5]. As observable from Fig. 10a, in case of no entry constraints, i.e. $K_2 = N_2 = 0.5$, the system can only converge to the segregation equilibrium Q_2 for low levels of tolerance of the local population, i.e. $\tau_1 < \widetilde{\tau}_1$ with $\tau_2^{SN}(\widetilde{\tau}_1, 1, 0.5) = 3.5$, and to cycles of different periods or chaotic attractors for $\tau_1 > \widetilde{\tau}_1$. It is worth noting that if a policymaker decides to impose an entry constraint for the newcomers, i.e. $K_2 < N_2$, as K_2 decreases, i.e. the entry limitation becomes more and more stringent, the blue region reduces and stable cycles of different periods undergo a sequence of border collision bifurcations that lead to a stable 2-cycle for sufficiently low level of K_2. Moreover, the gray region, representing the stability of the artificial equilibrium of non-segregation $\overline{P}_+$, appears for sufficiently low levels of tolerance of the member of the local population, i.e. for low levels of τ_1. The transition from the blue region, where the system converges to segregation, to the gray region, where the integration between the newcomers and the local population becomes feasible, provides indication of the effectiveness in increasing integration of the entry limitation policy. From the analysis of the 2D bifurcation diagram of Fig. 10b, we can conclude that limiting the number of newcomers allowed to enter a district can reduce the risk of segregation.

A similar analysis can be conducted varying τ_2 instead of τ_1. Such an investigation, for $\gamma = 1.5$, $N_2 = 0.5$ and $\tau_1 = 2$, is reported in Fig. 10c. From the figure it is possible to observe that without entry constraints the dynamics converge to one of the two fixed points of segregation Q_1 and Q_2 as indicated by the red region for both low and high levels of tolerance of the newcomers. In case of low levels of tolerance by newcomers, specifically for $\tau_2 < \tau_2^* = \frac{N_1}{N_2}$, the introduction of entry limitations cannot prevent segregation. This is obvious as limiting the number of newcomers allowed to enter the system has the same effect as reducing the level of tolerance of the members of this population. Indeed, in both cases the result is a lower number of newcomers entering the system. It follows that the entry limitations do not result to be useful in solving the problem of segregation if this is due to low levels of tolerance by the member of the population. On the contrary, for larger values of the levels of tolerance of the newcomers, i.e. for $\tau_2 > \tau_2^*$, the introduction of entry limitations for newcomers reduces the region of cycles or chaotic attractors and the region of segregation. Note that the red and white regions disappear as K_2 decreases. Moreover, the appearance of the gray regions indicates that an artificial fixed point of non-segregation is stable for certain values of K_2.

Regarding the constraint K_2, another interesting effect is its contribution in reducing chaos in the entry/exit dynamics of the system. For example, as observable from the phase

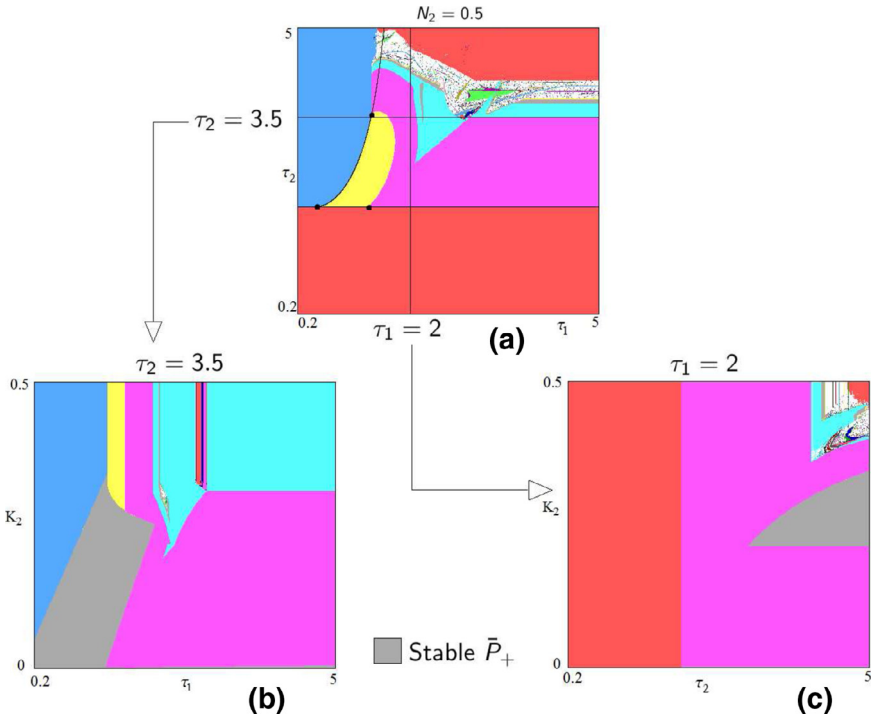

Fig. 10. Panel (a), 2D bifurcation diagram in the (τ_1, τ_2) parameter plane at $N_2 = K_2 = 0.5$, $\gamma = 1.5$ (as in Fig. 3b); Panel (b), 2D bifurcation diagram in the (τ_1, K_2) parameter plane $(\tau_1, K_2) \in [0.2, 5] \times [0, 5]$ at $\gamma = 1.5$ and $\tau_2 = 3.5$. Panel (c), 2D bifurcation diagram in the (τ_2, K_2) parameter plane $(\tau_2, K_2) \in [0.2, 5] \times [0, 5]$, with $\gamma = 1.5$ and $\tau_1 = 2$.

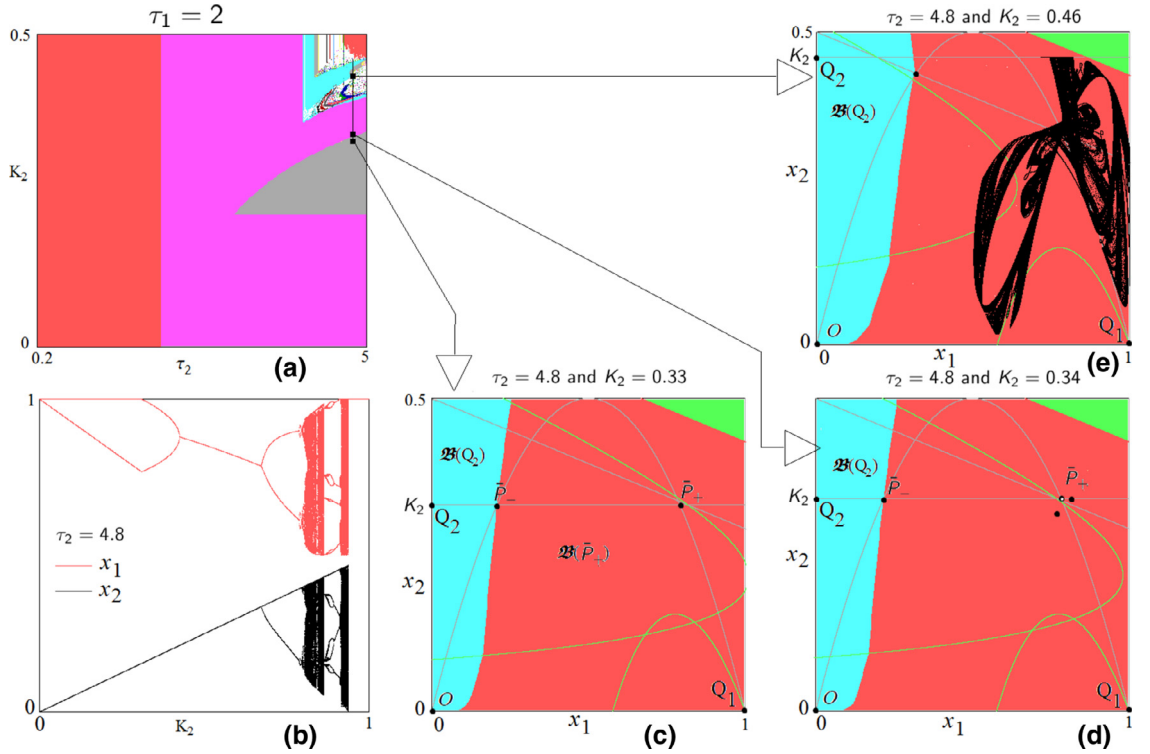

Fig. 11. Panel (a), 2D bifurcation diagram in the (τ_2, K_2) parameter plane as in Fig. 10c. Panel (b), 1D bifurcation diagram for $K_2 \in [0, 1]$ at $\tau_2 = 4.8$, $\tau_1 = 1$, $N_2 = 0.5$. Panels (c)–(e), phase plane $D = [0, 1] \times [0, K_2]$ for different levels of the entry limitation K_2. Transition from the stable equilibrium of non-segregation P_+ in panel (c), to a stable 2-cycle in panel (d) and to a chaotic attractor in panel (e).

spaces depicted in Fig. 11, the stable chaotic attractor of Fig. 11 b that exists for $K_2 = N_2$, disappears as K_2 decreases through a sequence of border collision bifurcations. Moreover, as K_2 is small enough, the artificial fixed point of non-segregation $\overline{P}_+$ becomes stable.

6. Conclusions

In this work we have analyzed in detail the global dynamics of a Schelling-type segregation model with heterogeneous distributions of tolerance similar to the one proposed in [10]. In particular, we have provided an accurate description of the conditions that lead to segregation. Among these, the most interesting is an excess of tolerance by members of the two groups involved, namely local population and newcomers. Then, these findings have been commented and discussed in terms of analogies and similarities with the ones emerging from the agent-base modeling, see, e.g., [7]–[9].

In addition, a further extension of the model is proposed by introducing entry-limitations for the newcomers as a policy measure to prevent segregation. The entry-limitation represents the maximum number of newcomers allowed to enter the system. By a combination of analytical results and numerical investigations we have discussed the effectiveness of this policy in preventing segregation. In particular, introducing the entry-restriction, we have found out that a fixed point of non-segregation can appear stable through a border collision bifurcation.

Other distributions of tolerance have been observed in empirical analysis, see e.g. [1], some of them characterized by a bimodal shape. An investigation of the model assuming these distributions of tolerance can reveal scenarios and dynamics not observable in this setting. This line of research is left for further studies.

Acknowledgments

This work has been performed under the auspices of COST Action IS1104 “The EU in the new complex geography of economic systems: models, tools and policy evaluation”. The second author also within the activities of the GNFM (INDAM Italian Research group).

References

[1] Clark WAV. Residential preferences and neighborhood racial segregation: a test of the Schelling segregation model. Demography 1991;28(1):1–19.
[2] Schelling TC. Models of segregation. Amer Econ Rev 1969;59(2):488–93.
[3] Schelling TC. Dynamic models of segregation. J Math Sociol 1971;1(2):143–86.
[4] Fossett M. Ethnic preferences, social distance dynamics, and residential segregation: theoretical explorations using simulation analysis. J Math Sociol 2006;30(3-4):185–274.
[5] Clark WAV, Fossett M. Understanding the social context of the Schelling segregation model. Proc Nat Acad Sci 2008;105(11):4109–14.
[6] Koehler G, Skvoretz J. Residential segregation in university housing: the mathematics of preferences. Soc Sci Res 2010;39(1):14–24.
[7] Epstein JM, Axtell RL. Growing artificial societies: social science from the bottom up. Brookings Institution Press; 1996.
[8] Gauvin L, Vannimenus J, Nadal JP. Phase diagram of a Schelling segregation model. Europ Phys J B-Condens Matter Complex Syst 2009;70(2):293–304.
[9] Zhang J. Residential segregation in an all-integrationist world. J Econ Behav Organ 2004;54(4):533–50.
[10] Bischi GI, Merlone U. Nonlinear economic dynamics; chap. In: An adaptive dynamic model of segregation. Nova Science Publisher; 2011. p. 191–205.
[11] Radi D, Gardini L, Avrutin V. The role of constraints in a segregation model: the symmetric case. Chaos, Solitons Fractals 2014;66:103–19.
[12] Radi D, Gardini L, Avrutin V. The role of constraints in a segregation model: the asymmetric case. Discr Dyn Nat Soc 2014 Article ID 569296, 17 pages. doi:10.1155/2014/569296.
[13] Nusse HE, Yorke JA. Border-collision bifurcations including “period two to period three” for piecewise smooth systems. Physica D 1992;57(1–2):39–57.
[14] Nusse HE, Yorke JA. Border-collision bifurcations for piecewise smooth one-dimensional maps. Int J Bifurcat Chaos Appl Sci Eng 1995;5(1):189–207.
[15] di Bernardo M, Budd CJ, Champneys AR, Kowalczyk P. Piecewise-smooth dynamical systems: theory and applications. Springer-Verlag; 2008.
[16] Zhusubaliyev ZT, Mosekilde E. Bifurcations and chaos in piecewise-smooth dynamical systems. World Scientific; 2003.
[17] Avrutin V, Futter B, Schanz M. The discontinuous top tent map and the nested period incrementing bifurcation structure. Chaos, Solitons Fractals 2012;45(4):465–82.
[18] Bischi GI, Gardini L, Merlone U. Impulsivity in binary choices and the emergence of periodicity. Discr Dyn Nat Soc 2009 Article ID 407913, 22 pages. doi:10.1155/2009/407913.
[19] Brianzoni S, Michetti E, Sushko I. Border collision bifurcations of superstable cycles in a one-dimensional piecewise smooth map. Math Comput Simul 2010;81(1):52–61.
[20] Bischi GI, Chiarella C, Kopel M, Szidarovszky F. Nonlinear oligopolies: stability and bifurcations. Springer-Verlag; 2010.
[21] Dal Forno A, Gardini L, Merlone U. Ternary choices in repeated games and border collision bifurcations. Chaos Solitons Fractals 2012;45(3):294–305.
[22] Gardini L, Merlone U, Tramontana F. Inertia in binary choices: continuity breaking and big-bang bifurcation points. J Econ Behav Organiz 2011;80(1):153–67.
[23] Gardini L, Sushko I, Naimzada A. Growing through chaotic intervals. J Econ Theory 2008;143(1):541–57.
[24] Hao BL. Elementary symbolic dynamics and chaos in dissipative systems. World Scientific; 1989.
[25] Hommes C, Nusse H. 'Period three to period two' bifurcation for piecewise linear models. J Econ 1991;54(2):157–69.
[26] Sushko I, Agliari A, Gardini L. Bifurcation structure of parameter plane for a family of unimodal piecewise smooth maps: border-collision bifurcation curves. Chaos, Solitons Fractals 2006;29(3):756–70.
[27] Sushko I, Gardini L, Matsuyama K. Superstable credit cycles and U-sequence. Chaos Solitons Fractals 2014;59:13–27.
[28] Tramontana F, Gardini L, Puu T. Mathematical properties of a combined Cournot-Stackelberg model. Chaos, Solitons Fractals 2011;44(1–3):58–70.
[29] Tramontana F, Gardini L, Westerhoff F. Heterogeneous speculators and asset price dynamics: further results from a one-dimensional discontinuous piecewise-linear map. Comput Econ 2011;38(3):329–47.
[30] Tramontana F, Westerhoff F, Gardini L. On the complicated price dynamics of a simple one-dimensional discontinuous financial market model with heterogeneous interacting traders. J Econ Behav Organ 2010;74(3):187–205.
[31] Sushko I, Gardini L. Degenerate bifurcations and border collisions in piecewise smooth 1D and 2D maps. Int J Bifurcat Chaos 2010;20(7):2045–70.
[32] Devaney RL. An introduction to chaotic dynamical systems. Allan M. Wylde; 1989.